J Cancer Res Clin Oncol
DOI 10.1007/s00432-015-1934-1

ORIGINAL ARTICLE – CANCER RESEARCH

Hypoxia-induced nitric oxide release by luminal cells stimulates proliferation and uPA secretion of myoepithelial cells in a bicellular murine mammary tumor

Martin Alejandro Krasnapolski · Catalina Lodillinsky · Elisa Bal De Kier Joffé · Ana María Eiján

Received: 23 January 2015 / Accepted: 5 February 2015

Abstract
Introduction LM38 murine mammary adenocarcinoma model is formed by LM38-LP (myoepithelial and luminal), LM38-HP (luminal) and LM38-D2 (myoepithelial) cell lines. In a previous work, we had shown that LM38-HP and LM38-D2 cell lines are less malignant than the bicellular LM38-LP cell line.
Purpose To study the role of nitric oxide (NO) as one of the mediators of functional interactions between malignant luminal and myoepithelial cells.
Methods and results Using immunohistochemistry, in vivo iNOS expression was only detected in the luminal cells of bicellular LM38-LP and most cells of LM38-HP tumors. In cobalt-induced pseudohypoxia, LM38-LP and LM38-HP cell lines significantly increased HIF-1α and iNOS expression (Western blotting) and therefore NO production (Griess method). This increase was inhibited by the iNOS inhibitor 1400 W. On the other side, NO was not detectable in LM38-D2 cells either in basal or in pseudohypoxia. In addition, pseudohypoxia increased urokinase-type plasminogen activator (uPA) secretion by LM38-LP and LM38-HP cells and migration in the LM38-LP cell line, without modulating these properties in LM38-D2 cells (radial caseinolysis). The NO donor DETA/NONOate (500 μM) was able to increase uPA secretion and in vitro growth of LM38-D2. In agreement, 1400 W prevented in vivo growth of the myoepithelial LM38-D2 cells.
Conclusions Hypoxia leads to an enhanced NO production by the luminal component, through HIF-1α and iNOS, which can stimulate myoepithelial cell proliferation and uPA secretion. In these new conditions, myoepithelial cells might act as an invasive forefront generating gaps that could help luminal cells to escape from the primary tumor.

Keywords Breast cancer · Myoepithelial cells · Luminal cells · Migration · Hypoxia · Nitric oxide

Elisa Bal De Kier Joffé and Ana María Eiján are Members of the Consejo Nacional de Investigaciones Científicas y Técnicas (CONICET).

M. A. Krasnapolski · C. Lodillinsky · E. Bal De Kier Joffé · A. M. Eiján (✉)
Área Investigación, Instituto de Oncología "Ángel H Roffo", Av. San Martín 5481, C1417DTB Buenos Aires, Argentina
e-mail: anamariaeijan@gmail.com

M. A. Krasnapolski
e-mail: mkrasnapolski@gmail.com

C. Lodillinsky
e-mail: catalina.lodillinsky@curie.fr

E. Bal De Kier Joffé
e-mail: balelisa2002@yahoo.com.ar

Present Address:
M. A. Krasnapolski
Departamento de patología, Instituto de Oncología "Ángel H Roffo", Buenos Aires, Argentina

Present Address:
C. Lodillinsky
Institut Curie Research Center, CNRS UMR 144, Paris, France

Introduction

The entire normal duct and lobular system of the mammary gland is composed of two epithelial cell types, present in roughly equal numbers: luminal cells that secrete milk, and an incomplete layer of myoepithelial cells that surrounds the inner layer and compresses it helping in milk expulsion. Currently, basal/myoepithelial cells function has been under reevaluation because their location between stroma and lumen makes them perfect candidates

Published online: 17 February 2015

to regulate physiological processes of the glandular epithelium as polarity, electrolyte and fluid flow and response to endocrine or paracrine signals (Lakhani and O'Hare 2001; Deugnier et al. 2002). Moreover, since the publication of the molecular classification of human breast cancer (Perou et al. 1999; Perou et al. 2000; Cancer Genome Atlas 2012), due to the worst prognosis shown by the basal-like tumors, more attention was gained by this cell type.

Myoepithelial cell contribution to carcinogenesis and tumor progression has recently begun to be recognized, and the literature is so far contradictory. While some studies have attributed great significance to the normal myoepithelium as a paracrine inhibitor of mammary cell proliferation and morphogenesis (Rudland et al. 1995; Liu et al. 1996), invasiveness (Xiao et al. 1999) and angiogenesis (Nguyen et al. 2000), and thus as an inhibitor of tumor progression (Sternlicht et al. 1997), in other systems, instead, myoepithelial cells were found to act as promoters of tumor growth (Gordon et al. 2003).

While in dogs, rats or mice, myoepithelial-cell-containing breast tumors are rather common (Rehm 1990), those are considered rare in human clinical practice, and the literature found is generally of small series or isolated cases (Santosh et al. 2013). However, myoepithelial cells have been found in tumors histopathologically classified as adenoid cystic carcinoma, adenosquamous carcinoma, adenomyoepithelioma and poorly differentiated myoepithelial-rich carcinoma. Furthermore, the contribution of myoepithelial cells to human ordinary ductal carcinomas is unclear. Interestingly, some reports suggest that 2–18 % of so-called *ductal carcinomas-no special type* shows focal or diffuse myoepithelial differentiation by immunohistochemical criteria (Nagle et al. 1986; Jones et al. 2001), and about 50 % of them follow an aggressive course (Foschini and Eusebi 1998).

Hypoxia is a very common phenomenon in the tumor microenvironment, especially in the first stages when tumors reach a volume that is too large for complete oxygen diffusion. The master regulator of the transcriptional response to hypoxia is the hypoxia-induced factor-1 (HIF-1), a member of the Per-ARNT-Sim (PAS) family of basic helix–loop–helix transcription factors (Wang et al. 1995). In normoxia, the α-subunit of HIF-1 (HIF-1α) is constitutively modified by Fe-containing hydroxylases in an oxygen-dependent fashion; hydroxylated HIF-1α is a target of the von Hippel–Lindau tumor suppressor, tagging HIF-1α for proteasomal degradation. In hypoxia, the low O_2 tension leads to the inability of HIF-1α hydroxylation, thus blocking its proteasomal degradation and causing its accumulation. Then, HIF-1α translocates into the nucleus, dimerizes with HIF-1β and binds to the hypoxia response element (HRE) (Fandrey et al. 2006), a consensus sequence found in promoters of several genes involved in multiple processes as metabolism, tissue remodeling, proliferation and gene expression (Le et al. 2004). Cobalt salts have the property to bind and inhibit Fe-hydroxylases generating *pseudohypoxia*, a condition in which, even in normoxia, there is detectable HIF-1 transcriptional activity (Wang and Semenza 1993).

One of the mechanisms co-opted by tumors to survive in a hypoxic atmosphere is the activation of the inducible nitric oxide synthase (iNOS) gene (Jung et al. 2000), an enzyme that produces high levels of nitric oxide (NO), which being a vasodilator, increases blood influx toward the tumor (Fukumura and Jain 1998). NO through a complex signaling mechanism (Thomas et al. 2008) is involved in many other processes as cell proliferation (Radisavljevic 2004), apoptosis prevention (Reveneau et al. 1999), migration and invasion (Jadeski et al. 2003), angiogenesis (Montrucchio et al. 1997) and immunosuppression (Hegardt et al. 2000), which can alter tumor progression (Lala and Orucevic 1998; Thomsen and Miles 1998).

Most of the studies addressing breast cancer development mechanisms are carried out with animal models that, although extremely useful, have some characteristics that may preclude the extrapolation of results to the human disease (Cardiff et al. 2000). Among them, pure cell lines disregard the interactions among the different cellular populations present in the most tumors (Hanahan and Weinberg 2011). In addition, it is noteworthy that murine mammary tumors do not usually metastasize to regional lymph nodes, one of the earliest and more frequent dissemination sites for human breast cancer, and the most significant prognostic factor predicting patient survival (Fisher et al. 2001).

Several years ago, a spontaneous transplantable mammary adenocarcinoma (M38), showing the capacity to metastasize both to lung and to draining lymph nodes, arose in our BALB/c colony (Bumaschny et al. 2004). M38 is a hormone-independent tumor, not expressing either the estrogen receptor or the epidermal growth factor receptor-related protein 2 (Erbb2). From this tumor, three cell lines have been generated: the bicellular cell line LM38-LP, constituted by islets of luminal cells surrounded by myoepithelial cells; the myoepithelial LM38-D2 cell line obtained by limiting-dilution cloning of LM38-LP cell line; and the nearly pure epithelial-like LM38-HP cell line. The lineage of the cells was confirmed by immunocytochemical expression of E-cadherin, alpha-type smooth muscle actin (α-SMA) and cytokeratins (CK) (Bumaschny et al. 2004).

In vivo, LM38-LP cells formed differentiated papillary adenocarcinomas composed of myoepithelial cells, positive for α-SMA, and CK-positive luminal cells surrounding fibrovascular strands. In contrast, the LM38-HP cells formed poorly differentiated adenocarcinomas with low CK expression and no evidence of glandular structures or α-SMA expressing cells. The LM38-D2 cells grew as an

undifferentiated tumor consisting of large spindle cells, positive for CK14 and α-SMA (Bumaschny et al. 2004).

Compared with the bicellular cell line and the parental M38 tumor, LM38-HP and LM38-D2 cell lines had a diminished in vivo growth rate, were significantly less metastatic to lung and only occasionally colonized the draining lymph node (Bumaschny et al. 2004). Our hypothesis is that the differentiated histopathology and pathogenic behavior depend on the interplay between both cell types. In the present work, we describe different studies conducted to dissect some of the biological and molecular bases that underlie their interaction.

Materials and methods

Immunohistochemistry

Formalin-fixed, paraffin-embedded sections from subcutaneous (s.c.) LM38-LP, LM38-HP and LM38-D2 tumors were used to analyze in vivo iNOS expression. Immunohistochemical staining was performed using an avidin–biotin–peroxidase complex (ABC, DAKO) according to manufacturer's instructions. iNOS (AbCam 15323) antibody was used at 1:200 dilution.

Cell culture

The bicellular (luminal and myoepithelial) LM38-LP, the myoepithelial clone LM38-D2 and the luminal-like LM38-HP cell lines were used (Bumaschny et al. 2004). All cell lines were cultured at 37 °C in a 5 % CO_2 humidified atmosphere and maintained in complete medium: Dulbecco's modified Eagle medium/nutrient mix F-12 (D-MEM/F-12) without HEPES (Gibco BRL, 12500-062) supplemented with gentamicin and 10 % FBS (GEN, Buenos Aires, Argentina) and subcultured every 3–4 days. The absence of mycoplasma contamination was routinely determined by 45-min staining with 1 μg/ml bisbenzimide (Höechst 33258) dye (Sigma, B 1155) and subsequent observation with fluorescence microscopy.

Nitric oxide release measurement

Cells were seeded in the internal 60 wells of 96-well plates with complete medium, and the peripheral 36 wells were filled with 200 μl PBS to avoid evaporation. When monolayers reached 80 % confluence, medium was changed with the addition of 2 mM L-arginine (Fluka, 11010) and with or without 150 μM cobalt(II) chloride (Fluka, 60818) to generate pseudohypoxia and/or 5 μM 1400 W (Calbiochem, 100050) a specific iNOS inhibitor. Plates were sealed to avoid external NO contamination, and after 24-h incubation, conditioned media were collected. Since NO is spontaneously transformed to nitrite, NO release was estimated as nitrite accumulation in the conditioned medium, compared with a sodium nitrite standard curve, using a modification of the Griess method (Xu et al. 2000), a chemical assay based on the observation that the adduct of nitroxides and sulfanilic acid (Fluka, 86090) interacts with N-(1-naphthyl) ethylenediamine (Sigma, N 5889) in an acidic pH, generating a product that is readily monitored by spectrophotometry with a 450-nm absorbance peak (Eijan et al. 2002).

Protein extraction

Cells were seeded in 100-mm culture dish and cultured until monolayers reached 80 % confluence. Then, they were washed three times with PBS and scrapped with a rubber policeman. After a soft centrifugation, cells were lysed with 1 % Triton X-100 (Biopack, 9002-93-1) in PBS supplemented with a protease inhibitor cocktail (Sigma, P 2714) for 45 min in ice. Then, protein extract was separated from cellular debris by a 15-min centrifugation at 15,000 RPM at 4 °C, aliquoted and kept at −20 °C. Protein concentration was quantified by Bradford assay (BioRad, 500-0006).

Western blotting

Protein extracts (80 μg) were resolved on SDS-PAGE (%T: iNOS, 7.5 % and HIF-1α, 9 %) and transferred to PVDF. Membranes were blocked for 1 h at room temperature in blocking buffer: 5 % skimmed milk in PBS + 0.1 % Tween 20 (PBS-T), and then incubated overnight at 4 °C with the following primary antibodies: iNOS (Santa Cruz Biotechnology, sc-8310), HIF-1α (Sigma, H 6536) or β-Actin (Sigma, A 4700) diluted 1:200, 1:1000 and 1:20,000, respectively, in blocking buffer. After washing three times for 10 min each time with PBS-T, the membranes were incubated for 1 h at room temperature with horseradish peroxidase-linked secondary antibodies diluted in blocking buffer: anti-mouse IgG (Sigma, A 9917) 1:20,000 and anti-rabbit IgG (Sigma, A 9169) 1:10,000. Then, membranes were washed three times for 10 min each time with PBS-T, and the signal was developed using Amersham ECL Western Blotting Detection Reagents (GE Healthcare, RPN 2134) according to manufacturer's instructions.

Total RNA extraction and RT-PCR

Cells were seeded in 60-mm culture dish and cultured until monolayers reached 80 % confluence. Then, they were subjected to different treatments, and total RNA was prepared with TRIzol reagent (Invitrogen, 15596-026)

according to manufacturer's directions. Agarose (Sigma, A5093) gel electrophoresis stained with GelGreen (Biotium, 41005) was used to evaluate the quality of the samples, and RNA was quantified using a Qubit fluorometer (Invitrogen, Q32857) according to manufacturer's instructions. Then, first-strand cDNA was synthesized with the iScript cDNA synthesis kit (BioRad, 170-8890) according to manufacturer's instructions using 500 μg RNA as a source. One microliter cDNA was used as a template for PCR amplification in a Mastercycler personal (Eppendorf, 5332 000.014) using specific primers for iNOS or β-actin, recombinant *Taq* DNA polymerase kit (Invitrogen, 10342-020) and dNTP mix (Invitrogen, 18427-013). Controls for the absence of genomic DNA contamination were obtained by performing the amplification reaction with RNA samples previously to retrotranscription, and the absence of self-priming was assessed by performing the amplification reaction in the absence of template.

Primers and PCR programs

The primers for the iNOS mRNA were iNOS-F: 5′-CTC ACTGGGACAGCACAGAA-3′ and iNOS-R: 5′-TGGTC AAACTCTTGGGGTTC-3′ and for the β-actin mRNA β-actin-F: 5′-GTGGGCCGCTCTAGGCACCA-3′ and β-actin-R: 5′-CGGTTGGCCTT AGGGTTCAGGGGGG-3′. For iNOS mRNA, 36 cycles of amplification were performed with denaturation (94 °C for 1 min), annealing (58 °C for 1 min) and elongation (72 °C for 1 min), followed by a final elongation (72 °C for 5 min). For β-actin mRNA, amplification was as above, but the annealing step was done at 62 °C. The PCR-amplified products were visualized by agarose (Sigma, A5093) gel electrophoresis stained with GelGreen (Biotium, 41005).

Immunofluorescence

Cells were seeded on cell culture-treated coverslips in 24-well plates and cultured with complete medium. When monolayers reached 80 % confluence, medium was changed with or without treatment (150 μM $CoCl_2$). After 30 min, 3 or 16 h, each well was fixed with 4 % formaldehyde/PBS for 15 min and washed two times with PBS. Then, cells were permeabilized with 20-min incubation with 1 % Triton X-100/PBS at 37 °C, then blocked for 1 h at room temperature in blocking buffer (1 % FBS in PBS) and then incubated overnight at 4 °C with the primary antibody, HIF-1α (Sigma, H 6536) diluted 1:50 in blocking buffer. After washing with PBS, coverslips were incubated 1 h at room temperature with a FITC-linked secondary antibody rabbit anti-mouse IgG (Zymed, 81-6711) diluted 1:100 in blocking buffer. After washing with PBS, coverslips were mounted, observed and photographed with an epifluorescence microscope (Nikon Eclipse E400).

In vitro NO susceptibility assay

Cells were seeded in 96-well plates and cultured with complete medium. When monolayers reached 80 % confluence, medium was changed and different concentrations of the NO donor DETA/NONOate (DETA) (Cayman, 82120) were added. After 24-h incubation, cell number in each well was estimated using CellTiter 96® AQ_{ueous} non-radioactive cell proliferation assay (MTS) (Promega, G5421) according to manufacturer's instructions.

Wound healing assay

Cells were seeded in 35-mm culture dish and cultured with complete medium. When monolayers reached 100 % confluence, three parallel wounds were made with a 200-μl pipette tip (approximately 400 μm wide); each wound was photographed in three random microscopic fields, and the initial area was measured using the free software Image J 1.42q (National Institutes of Health, Bethesda, Maryland, USA, http://imagej.nih.gov/ij/). After 16 h, the same fields were photographed and the migratory capacity was calculated as the difference of the cell-free area in each field.

Urokinase-type plasminogen activator activity assay

Secreted urokinase-type plasminogen activator (uPA) activity was determined in conditioned medium as described previously (Urtreger et al. 1999). Caseinolytic uPA activity was referenced to a urokinase standard curve (range 0.1–10 IU/ml) and normalized to cell protein content.

In vivo tumor growth

To assess the effect of NO on the early stages of tumor formation, we used the following short-term in vivo assay. Briefly, 8-week-old syngeneic female BALB/c mice were inoculated intradermally (i.d.) with 2×10^5 cells in 0.1 ml DMEM/F-12 without FBS and with (left flank) or without (right flank) 5 μM 1400 W (Calbiochem, 100050), a specific iNOS inhibitor (Garvey et al. 1997). Five microliters of trypan blue (Sigma, T 6146) was added to mark the inoculation site. After 5 days, mice were killed by CO_2 inhalation, the dermis section corresponding to the injection site was dissected, and tumors were photographed and measured with the free software Image J 1.42q (National Institutes of Health, Bethesda, Maryland, USA, http://imagej.nih.gov/ij/).

Ethics statement

Mice, from the Animal Facility of the Institute of Oncology "Angel H. Roffo" (Buenos Aires, Argentina), were handled in accordance with the international procedure for Care and Use of Laboratory Animals. (EU Directive 2010/63/EU for animal experiments). In vivo protocols were approved by the Institutional Review Board CICUAL, protocol number 2012/02, Institute of Oncology "Angel H. Roffo."

Statistical analysis

All experiments were performed at least in triplicate. The differences were studied by ANOVA with Bonferroni contrasts. Differences between proportions in the in vivo assay were analyzed by Chi-square test. A value of $p < 0.05$ was considered to be significant.

Results

Only luminal cells express iNOS in vivo and release nitric oxide in vitro

Since NO is a very important mediator in tumor biology, we explored by immunohistochemistry the expression of iNOS, enzyme responsible for the highest NO levels, in tumors formed after the s.c. inoculation of the different cell lines of the LM38 model.

Figure 1a shows that iNOS-positive luminal cells and iNOS-negative myoepithelial ones could be recognized in the papillary adenocarcinoma grown from the bicellular LM38-LP cell line. In the same sense, we found that poorly differentiated luminal-like cells comprising the LM38-HP tumors were positive for iNOS, while the myoepithelial cells constituting LM38-D2 tumors did not express the enzyme.

Given that hypoxia is a common phenomenon in the tumor microenvironment and is a major iNOS inductor, we evaluated NO production in vitro in control and in cobalt-induced *pseudohypoxia* conditions. Figure 1b shows that the bicellular LM38-LP cell line and the luminal LM38-HP one presented a basal release of NO. A treatment with 150 μM cobalt(II) chloride ($CoCl_2$) significantly increased LM38-LP and LM38-HP NO production. In LM38-LP cells, both the basal and the $CoCl_2$-stimulated NO release were completely blocked by 1400 W, a specific iNOS inhibitor (Garvey et al. 1997). On the other hand, in LM38-HP cells, 1400 W only inhibited

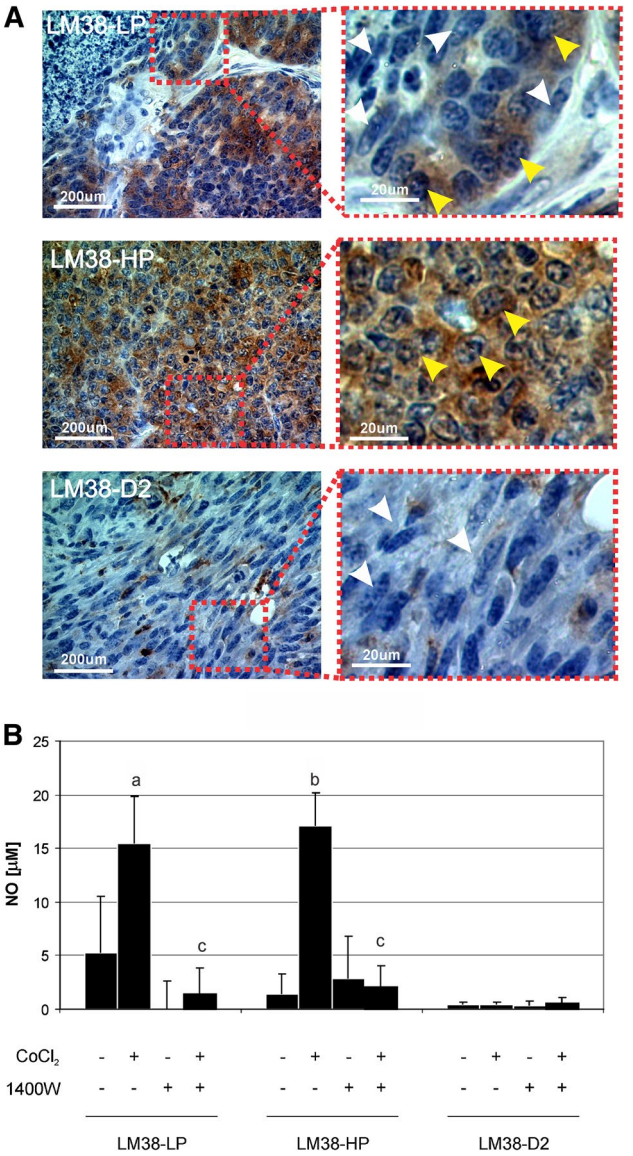

Fig. 1 In vivo iNOS expression and in vitro nitric oxide production. **a**: Immunohistochemistry for iNOS in s.c. tumors of the different cell lines. *Left panels*: ×400 microphotographs; *right panels*: ×10 magnifications of the selected areas. LM38-LP tumor shows iNOS-positive luminal cells (*yellow arrowhead*) and iNOS-negative myoepithelial cells (*white arrowhead*). Most LM38-HP tumor cells are positive for iNOS, while most LM38-D2 tumor cells are negative for this enzyme. Regarding cell morphology, *right panel* shows that LM38-HP is similar to the luminal cells (*yellow arrowhead*) and LM38-D2 is similar to the myoepithelial cells (*white arrowhead*), of LM38-LP tumor. **b**: Griess assay was done to evaluate nitric oxide (NO) release from LM38-LP, LM38-HP and LM38-D2 cells in basal conditions, in $CoCl_2$-induced pseudohypoxia, and with 5 μM 1400 W. LM38-LP and LM38-HP, but not LM38-D2 cells produced detectable NO levels. Pseudohypoxia significantly increased NO production in LM38-LP and LM38-HP but not in LM38-D2 (*a*: $p < 0.05$; *b*: $p < 0.01$ vs. untreated cells). 1400 W almost completely blocked NO production (*c*: $p < 0.01$ vs. $CoCl_2$ treated cells)

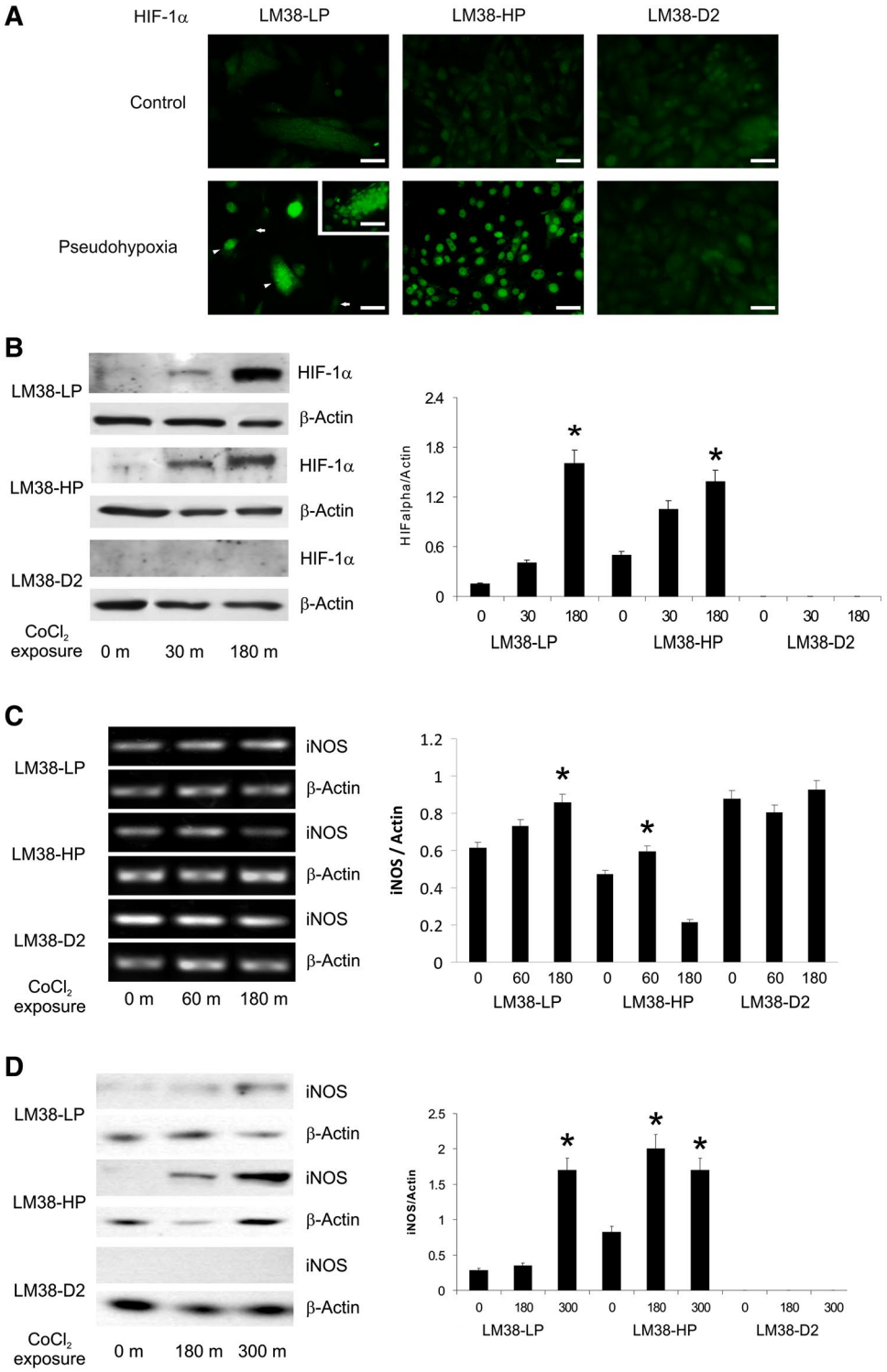

Fig. 2 In vitro HIF-1α and iNOS expression. **a** Immunofluorescence for HIF-1α shows nuclear localization in LM38-LP and HP cells in pseudohypoxia. No nuclear HIF-1α expression was detected in LM38-D2 cell line either basally or under $CoCl_2$ treatment. In LM38-LP cells in pseudohypoxia, *white arrows* point to negative myoepithelial nuclei and *white arrowheads* point to positive luminal islets. Insert: Magnification of a luminal islet showing HIF-1α nuclear expression. **b** Representative Western blots (*left panel*) showing induction of HIF-1α protein by $CoCl_2$ in LM38-LP and LM38-HP ($^*p < 0.01$vs. T_0) but not in LM38-D2 cells. **c** Representative RT-PCR assay (*left panel*) showing that iNOS-mRNA expression was induced at 60 min after $CoCl_2$ treatment in LM38-LP and HP cells ($^*p < 0.05$ vs. T_0). Constitutively high iNOS-mRNA levels were detected in LM38-D2 cells that were not modulated by $CoCl_2$ **d** Representative Western blots (*left panel*) showing increased iNOS protein in LM38-LP and HP cells after $CoCl_2$ treatment ($^*p < 0.01$ vs. T_0). No iNOS protein was detected in LM38-D2. The B, C and D *right panels* show densitometric quantitation, relative to β-actin, for HIF-1α, iNOS mRNA and iNOS protein, respectively

the $CoCl_2$-stimulated NO release. Myoepithelial LM38-D2 cells did not release detectable NO either basally or in pseudohypoxia, coincidently with the in vivo absence of iNOS expression. Together, these results suggest that iNOS is responsible of NO release induced by pseudohypoxia in luminal cells.

Only luminal cells respond to hypoxia increasing HIF-1α and iNOS

Since upon stabilization HIF-1α translocates to the cell nucleus, immunofluorescence was performed to analyze the intracellular localization of HIF-1α post-$CoCl_2$ treatment.

Figure 2a shows that HIF-1α was undetectable in basal conditions, while in pseudohypoxia, it could be detected in the nuclei of the luminal cells of the bicellular LM38-LP cell line (white arrowheads) and in the nuclei of LM38-HP cells. On the other hand, neither the myoepithelial component of LM38-LP cell line (white arrows) nor LM38-D2 cells expressed HIF-1α in any culture condition. In concordance, Western blotting also showed an increase in HIF-1α protein, only in LM38-LP and LM38-HP cell lines. This increase was detected as early as 30 min and continued at least for 3 h post-treatment with $CoCl_2$ (Fig. 2b). Since LM38-LP and LM38-HP cell lines were able to produce NO in pseudohypoxia and iNOS is a HIF-1α target gene, RT-PCR was performed to evaluate the status of iNOS mRNA in this condition. Figure 2c shows that iNOS mRNA was increased in LM38-LP and LM38-HP cell lines at 60 min post-$CoCl_2$, remaining unchanged in LM38-D2 cells. In the same sense, the expression of iNOS at protein level analyzed by Western blot showed an increase at 3 h post-treatment in the luminal-cell-containing cell lines LM38-LP and LM38-HP, while in LM38-D2 cell line this molecule was undetectable (Fig. 2d).

Pseudohypoxia increases the migratory capacity of the bicellular cell line

Wound migration assays were performed to study the migratory ability of the different cell lines in basal and pseudohypoxia conditions. As shown in Fig. 3a, b, in control conditions LM38-D2 cells presented the highest migratory capacity and LM38-HP epithelial cells were poorly migratory. Interestingly, in the bicellular cell line LM38-LP, only myoepithelial cells migrated into the wound (Fig. 3a, white arrow). On the other hand, pseudohypoxia induced by $CoCl_2$ increased the migratory ability of only the bicellular LM38-LP cell line.

Nitric oxide increased secreted uPA activity in LM38-D2 cell line, while pseudohypoxia did so in LM38-LP and LM38-HP cell lines

The serine protease uPA initiates an enzymatic cascade involving the activation of plasminogen to plasmin and of metalloproteinases (MMPs), which not only enables the degradation of the surrounding extracellular matrix but also may exert other roles in regulating cell proliferation and migration among others (Margheri et al. 2014). Previously, we had found that the three cell lines did not differ in the capacity to secrete MMP-9, while LM38-LP cells showed higher uPA activity than LM38-HP and LM38-D2 (Bumaschny et al. 2004). Thus, this enzyme seemed to be more relevant to analyze its modulation by NO and under hypoxic conditions. Therefore, we evaluated the activity

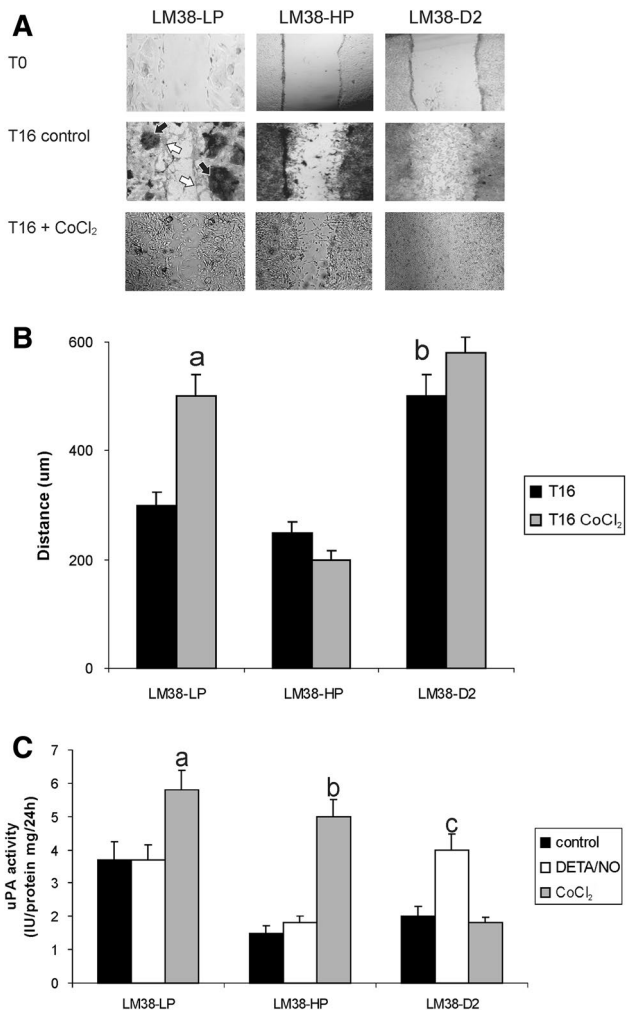

Fig. 3 Migration and uPA secretion. **a** Representative microphotographs of the initial time (T_0) and after 16 h of migration (T16) with or without $CoCl_2$ of the wound migration assays of LM38-LP, LM38-HP and LM38-D2 cell lines. In the LM38-LP cell line, it can be seen that the myoepithelial cells (*white arrow*) show the higher migratory capacity, entering the wound by surrounding the epithelial islets (*black arrow*). **b** Quantification of the migratory ability of the different cells, indicating the average distance covered by each cell type. LM38-D2 cells were significantly more migratory than LM38-LP and LM38-HP (*b*: $p < 0.01$). $CoCl_2$ enhanced the migration of LM38-LP (*a*: $p < 0.01$ vs. untreated cells). **c** Radial caseinolysis was performed with conditioned media of LM38-LP, LM38-HP and LM38-D2 cells either basally or in the presence of 150 μM $CoCl_2$ or 500 μM DETA. Pseudohypoxia increased uPA secreted activity of LM38-LP and LM38-HP cells, while NO increased uPA secreted activity only in LM38-D2 cells (*a* and *c*: $p < 0.05$ vs. respective untreated cells; *b*: $p < 0.01$ vs. LM38-HP untreated cells)

of uPA in conditioned media from the different cell lines treated with DETA (500 μM) or with $CoCl_2$ (150 μM). Figure 3c shows that the pseudohypoxic condition increased uPA activity in LM38-LP and LM38-HP cells, while it did not affect uPA secretion by LM38-D2 cells. On the other hand, exogenous NO only increased uPA activity in

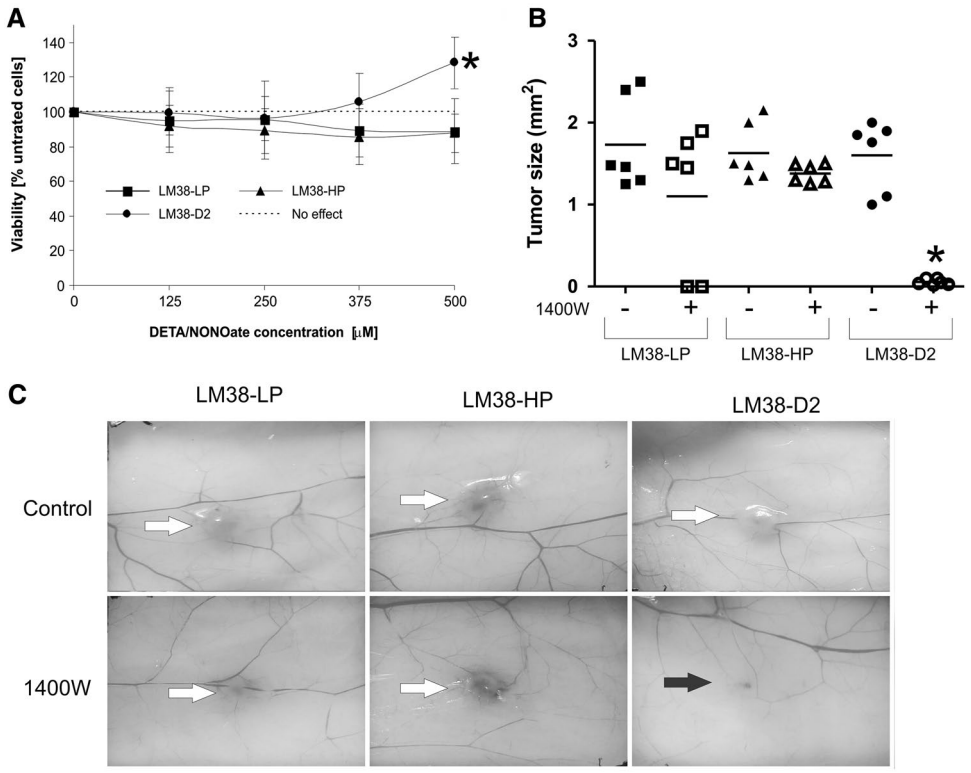

Fig. 4 Effect of NO on in vitro proliferation and of iNOS inhibition on in vivo tumor growth. **a** In vitro estimation of the proliferation of LM38-LP, LM38-HP and LM38-D2 cell lines in the presence of a NO donor by MTS assay. DETA (500 μM) significantly increased LM38-D2 cells proliferation (*: $p < 0.05$) relative to control cells. **b** and **c** In vivo tumor growth of the three cell lines with or without 5 μM 1400 W. **b** Size of LM38-LP, LM38-HP and LM38-D2 tumors in the presence of a NO inhibitor. *Scatter plot* showing individual tumor size, *horizontal lines* represent the group means size. Only LM38-D2 growth was significantly inhibited by 1400 W (* $p < 0.05$ vs. untreated cells). **c** Microphotographs showing representative tumors (*white arrow*). No tumor was developed by LM38-D2 cells in the presence of 1400 W (*black arrow* shows inoculation site)

LM38-D2 cells. These results suggest the role of uPA in the increase of the migratory ability of LM38-LP cells under pseudohypoxia, regulated at least in part by NO production.

NO increased in vitro proliferation of myoepithelial LM38-D2 cells and is necessary for their in vivo growth

To evaluate the effect of NO on the proliferation of the different cell lines, cells were treated in vitro with increasing concentrations of DETA for 24 h. Figure 4a shows that while, at any dose, DETA did not affect the proliferation of the bicellular LM38-LP and the luminal LM38-HP cell lines, we could observe a 30 % increase in LM38-D2 cell number at 500 μM, indicating that NO might act as a mitogen for myoepithelial cells.

To evaluate whether NO was also necessary for in vivo growth, LM38-LP, LM38HP and LM38-D2 cells were inoculated intradermal (i.d.) into the flanks of syngeneic BALB/c mice with or without 5 μM 1400 W. Figure 4b shows the size of the individual tumors and the average of each group, and Fig. 4c illustrates representative tumors analyzed. All cell lines developed tumors in 100 % of mice in basal conditions. Interestingly, 100 % of the mice inoculated with LM38-HP cells + 1400 W developed i.d. tumors, versus only 66.6 % of those injected with LM38-LP + 1400 W, furthermore no tumor was formed when LM38-D2 cells were co-inoculated with the iNOS inhibitor (Fig. 4b). Since 1400 W could only significantly impair the in vivo growth of LM38-D2 (Fig. 4b, c), we could suggest that NO is also necessary for in vivo growth of myoepithelial cells.

Discussion

Malignant myoepithelial cell role during tumor progression is a very controversial topic. While some authors (Barsky and Karlin 2005, 2006) have attributed them a suppressing role, others have recognized that myoepithelial cells can promote a metastatic phenotype (Adriance et al. 2005). This apparent contradiction can be explained since the first works were made using transformed myoepithelial cells

derived from benign tumors and not actual malignant cells. The LM38 adenocarcinoma model formed by luminal and myoepithelial malignant cells is suitable to study the heterotypic interactions between different cell compartments that confer tumors their malignant phenotype (Bumaschny et al. 2004).

In the first stages of tumor growth, when tumor size exceeds the distance reached by oxygen diffusion, and an angiogenic response has not already been mounted, cells suffer a transient hypoxia period that triggers, among other biological effects, the release of NO (Sollid et al. 2006). We could show a relationship between in vivo iNOS expression in tumors and the cellular capacity for in vitro NO release. The study of iNOS expression by immunohistochemistry in sections of the different tumors revealed that only luminal cells, either from LM38-LP or from LM38-HP tumors, were positive for the enzyme. In agreement with this finding, in vitro, LM38-HP luminal cells could release NO basally and increased its levels in response to pseudohypoxia. Besides, LM38-D2 myoepithelial cells were negative for in vivo iNOS expression and could not release NO in vitro, either in basal or in pseudohypoxia conditions.

Molecular events underlying the response to hypoxia are regulated by the heterodimeric transcription factor HIF. Here, we show that luminal cells in response to hypoxia activate the HIF-1α/iNOS pathway. HIF-1α was increased in the luminal-cell-containing cell lines LM38-LP and LM38-HP after 30 min of pseudohypoxia induction. Furthermore, while HIF-1α and iNOS protein levels were increased in luminal cells upon $CoCl_2$ treatment, myoepithelial cells seemed unable to sense pseudohypoxia. This correlated with the lack of expression of HIF-1α and iNOS proteins by these cells. In concordance with protein expression, iNOS mRNA only was increased in the cell lines that contain luminal cells. Surprisingly, although iNOS mRNA was present in LM38-D2 cells, it was not modulated by pseudohypoxia. Although we do not know why iNOS protein is not expressed in LM38-D2 cells, in which otherwise iNOS mRNA is present, it is possible that posttranscriptional mechanisms are involved in this apparently contradictory result.

The role of NO in tumor biology is controversial, because it can be either cytotoxic or promote survival, depending on the concentration and on different aspects of the cellular context and the microenvironment (Ridnour et al. 2008). Aberrant expression of iNOS was observed in 61 % of 161 malignant human breast tumors and showed a positive correlation with clinicopathological features associated with a bad prognosis, including tumor size and overall survival (Loibl et al. 2005). More recently, among poor outcome estrogen-receptor-negative breast tumors, iNOS expression was described as a marker of a subgroup with an even worst survival (Glynn et al. 2010).

In our system, we have shown that luminal–myoepithelial interactions, via NO, induce a proliferative state that leads to tumor growth. In vitro, myoepithelial cells had a direct proliferative response to NO. To evaluate the in vivo relevance of hypoxia and NO in the first stages of tumor development, we designed a short-term growth experiment where tumor cell lines were inoculated intradermally with or without the iNOS-specific inhibitor 1400 W in different flanks of the same animal. We cannot exclude that a small amount of 1400 W could disperse by blood and, in consequence, affect the tumor on the other flank. However, since tumor growth was indeed significantly different between both treatments, this does not seem to be the case. None of LM38-D2-inoculated mice and only two-thirds of LM38-LP-inoculated mice could form tumors in the presence of 1400 W, suggesting that NO is important for the growth of the myoepithelial-cell-containing tumors. Taking into account that iNOS expression at protein level was absent in LM38-D2 cells, we could infer that the actual target of 1400 W was stromal cells, such as macrophages, that released NO in response to the presence of the tumor cells (Solinas et al. 2009), or endothelial cells that released NO via HIF-1α/iNOS in response to a transient hypoxic state (Branco-Price et al. 2012).

There are evidences that hypoxia through HIF-1α induction is associated with epithelial to mesenchymal transition and the production of proteolytic enzymes, among other processes that lead to tumor progression and metastasis (Chen et al. 2010). It was described that migration of tumor cells during hematogenous metastasis is related to a HIF-driven response (Liao et al. 2007). Malignant myoepithelial cells are very migratory and invasive (Williams-Fritze et al. 2011), an attribute already present in their non-tumorigenic counterpart (Gordon et al. 2003) that allows them to easily escape from primary tumors for generating a secondary growth. LM38-D2 cells were more migratory than LM38-HP and LM38-LP cell lines. Even more, an increase of the migratory ability of LM38-LP cells was detected under pseudohypoxia. Since we have shown that myoepithelial cells are the main responsible for the in vitro wound closure and that these cells cannot sense hypoxia, we can assume that the interaction with the luminal cells leads to this increase in migration. Several proteolytic enzymes, such as uPA, have been associated with migration ability.

We have previously shown that LM38-D2 malignant myoepithelial cells secrete high levels of proteases, including uPA (Bumaschny et al. 2004). While uPA secretion was basally high in all three cell lines, its increase was triggered differentially in the bicellular LM38-LP and the luminal-like LM38-HP cell lines, compared with the myoepithelial clone LM38-D2. Pseudohypoxia increased uPA secreted activity of LM38-LP and LM38-HP cells, while NO increased uPA secreted activity only in LM38-D2 cells.

These results are consistent with the hypothesis that NO produced by luminal cells in hypoxia is, in part, responsible for the increase of uPA secretion by the myoepithelial cells. On the other hand, the bicellular and the luminal cell lines, that have the capacity to release NO, were insensitive to exogenous NO. However, in pseudohypoxia, these cell lines could increase uPA secretion possibly by a NO-independent mechanism, since 1400 W was unable to inhibit this uPA increase (data no shown). A close relationship between hypoxia, uPA and tumor progression was also described in gastric tumors since an antibody against uPA could inhibit hypoxia-induced invasive ability (Liu et al. 2010).

Malignant myoepithelioma of the breast is a human neoplasm composed exclusively of myoepithelial cells. This is a very rare tumor, and only few cases are reported in the literature (Santosh et al. 2013). It was described that normal myoepithelial cells are mitotically quiescent with a low proliferative index (Joshi et al. 1986). It may be possible that the low frequency of occurrence of these human tumors is associated with a low growing capacity of malignant myoepithelial cells, allowing tumors to remain in a state of latency and not be clinically detected. In the same way, the in vivo inoculation of LM38-D2 rendered tumors resembling human myoepithelial carcinomas with low growth potential (Bumaschny et al. 2004). In consequence, the LM38-D2 cell line is a good model to understand the biological behavior of these human tumors. Therefore, malignant myoepithelial cells probably require the cooperation of other cells such as malignant luminal cells in order to express their aggressive potential. In this sense, our results show a model of cooperation between malignant luminal and myoepithelial cells. Thus, the malignant behavior of the tumor M38, composed of luminal epithelial and myoepithelial cells, may be explained by the following cooperative model (Fig. 5). The hypoxic conditions normally established at the initial stages of tumor growth lead, in the luminal compartment, to the enhancement of uPA activity and to the inhibition of HIF-1α degradation, its nuclear translocation and the induction of hypoxia-responsive genes in these cells. iNOS, a prototypic hypoxia-responsive gene, is also induced and NO is generated. This factor not only enhances uPA production in myoepithelial cells, but is also necessary for its in vivo migration, survival and proliferation. Myoepithelial cells, in turn, being very invasive (data not shown), act in a three-dimensional context as an invasive forefront, generating gaps in the basal membrane and the extracellular matrix that help luminal cells to abandon the primary tumor and disseminate to distant sites. Supporting this hypothesis, a recent paper by Cheung et al. (2013) using a three-dimensional model of invasion could demonstrate the importance of cells with basal differentiation in this process.

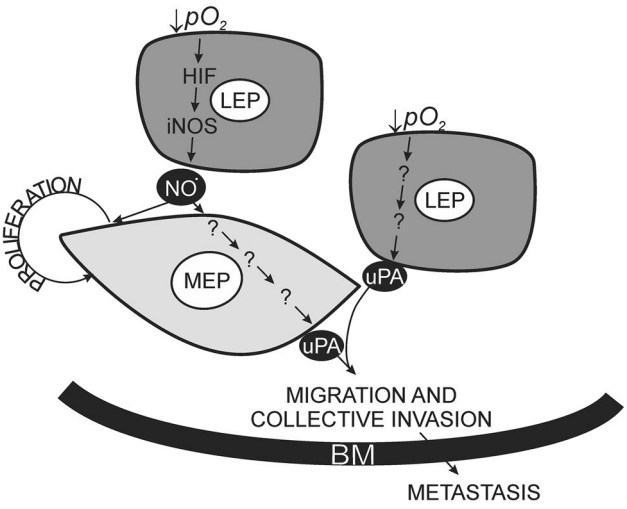

Fig. 5 Hypothetical collaborative model. Upon a low O_2 pressure (pO_2), luminal (LEP) cells sense hypoxia and increase uPA secretion and HIF-1α nuclear translocation and transcriptional activity. This induces iNOS expression, leading to NO release. This factor is necessary for myoepithelial (MEP) cells survival and proliferation, and also enhances their capacity to secrete uPA. MEP cells, being very migratory and invasive, generate gaps in the basement membrane (BM) and the extracellular matrix, which may be exploited by LEP cells to abandon the primary tumor and disseminate to distant sites

Together, our results show that NO gives an advantage that leads to tumor growth, thus being a poor prognosis factor for breast cancer patients. In consequence, iNOS could be regarded as a therapeutic target to basal/myoepithelial-cell-containing breast cancer.

Acknowledgments We would like to thank MSc Lina Marino, Alicia Rivelli and Silvina Romero for help with immunohistochemistry and technical assistance. Also, we are thankful to Vanina Rodriguez and Candela Martin for the provision and care of mice. This work was supported by Grants from the Agencia Nacional para la Promoción de la Ciencia y la Tecnolgía (ANPCyT, Prestamo BID PICT2010-01296), from the Universidad de Buenos Aires (UBACYT MO15 and M20020100100243) and from Concejo Nacional de Investigaciones Científicas y Técnicas (CONICET, PIP193). No founding source had any involvement in study design; the collection, analysis or interpretation of data; in the writing of the report; or in the decision to submit the article for publication.

Conflict of interest None.

References

Adriance MC, Inman JL, Petersen OW, Bissell MJ (2005) Myoepithelial cells: good fences make good neighbors. Breast Cancer Res 7(5):190–197

Barsky SH, Karlin NJ (2005) Myoepithelial cells: autocrine and paracrine suppressors of breast cancer progression. J Mammary Gland Biol Neoplasia 10(3):249–260

Barsky SH, Karlin NJ (2006) Mechanisms of disease: breast tumor pathogenesis and the role of the myoepithelial cell. Nat Clin Pract Oncol 3(3):138–151

Branco-Price C, Zhang N, Schnelle M, Evans C, Katschinski DM, Liao D, Ellies L, Johnson RS (2012) Endothelial cell HIF-1alpha and HIF-2alpha differentially regulate metastatic success. Cancer Cell 21(1):52–65

Bumaschny V, Urtreger A, Diament M, Krasnapolski M, Fiszman G, Klein S, Joffe EB (2004) Malignant myoepithelial cells are associated with the differentiated papillary structure and metastatic ability of a syngeneic murine mammary adenocarcinoma model. Breast Cancer Res 6(2):R116–R129

Cancer Genome Atlas N (2012) Comprehensive molecular portraits of human breast tumours. Nature 490(7418):61–70

Cardiff RD, Anver MR, Gusterson BA, Hennighausen L, Jensen RA, Merino MJ, Rehm S, Russo J, Tavassoli FA, Wakefield LM, Ward JM, Green JE (2000) The mammary pathology of genetically engineered mice: the consensus report and recommendations from the Annapolis meeting. Oncogene 19(8):968–988

Chen J, Imanaka N, Chen J, Griffin JD (2010) Hypoxia potentiates Notch signaling in breast cancer leading to decreased E-cadherin expression and increased cell migration and invasion. Br J Cancer 102(2):351–360

Cheung KJ, Gabrielson E, Werb Z, Ewald AJ (2013) Collective invasion in breast cancer requires a conserved basal epithelial program. Cell 155(7):1639–1651

Deugnier MA, Teuliere J, Faraldo MM, Thiery JP, Glukhova MA (2002) The importance of being a myoepithelial cell. Breast Cancer Res 4(6):224–230

Eijan AM, Piccardo I, Riveros MD, Sandes EO, Porcella H, Jasnis MA, Sacerdote De Lustig E, Malagrino H, Pasik L, Casabe AR (2002) Nitric oxide in patients with transitional bladder cancer. J Surg Oncol 81(4):203–208

Fandrey J, Gorr TA, Gassmann M (2006) Regulating cellular oxygen sensing by hydroxylation. Cardiovasc Res 71(4):642–651

Fisher ER, Anderson S, Tan-Chiu E, Fisher B, Eaton L, Wolmark N (2001) Fifteen-year prognostic discriminants for invasive breast carcinoma: national Surgical Adjuvant Breast and Bowel Project Protocol-06. Cancer 91(8 Suppl):1679–1687

Foschini MP, Eusebi V (1998) Carcinomas of the breast showing myoepithelial cell differentiation. A review of the literature. Virchows Arch 432(4):303–310

Fukumura D, Jain RK (1998) Role of nitric oxide in angiogenesis and microcirculation in tumors. Cancer Metastasis Rev 17(1):77–89

Garvey EP, Oplinger JA, Furfine ES, Kiff RJ, Laszlo F, Whittle BJ, Knowles RG (1997) 1400 W is a slow, tight binding, and highly selective inhibitor of inducible nitric-oxide synthase in vitro and in vivo. J Biol Chem 272(8):4959–4963

Glynn SA, Boersma BJ, Dorsey TH, Yi M, Yfantis HG, Ridnour LA, Martin DN, Switzer CH, Hudson RS, Wink DA, Lee DH, Stephens RM, Ambs S (2010) Increased NOS2 predicts poor survival in estrogen receptor-negative breast cancer patients. J Clin Invest 120(11):3843–3854

Gordon LA, Mulligan KT, Maxwell-Jones H, Adams M, Walker RA, Jones JL (2003) Breast cell invasive potential relates to the myoepithelial phenotype. Int J Cancer 106(1):8–16

Hanahan D, Weinberg RA (2011) Hallmarks of cancer: the next generation. Cell 144(5):646–674

Hegardt P, Widegren B, Sjogren HO (2000) Nitric-oxide-dependent systemic immunosuppression in animals with progressively growing malignant gliomas. Cell Immunol 200(2):116–127

Jadeski LC, Chakraborty C, Lala PK (2003) Nitric oxide-mediated promotion of mammary tumour cell migration requires sequential activation of nitric oxide synthase, guanylate cyclase and mitogen-activated protein kinase. Int J Cancer 106(4):496–504

Jones C, Nonni AV, Fulford L, Merrett S, Chaggar R, Eusebi V, Lakhani SR (2001) CGH analysis of ductal carcinoma of the breast with basaloid/myoepithelial cell differentiation. Br J Cancer 85(3):422–427

Joshi K, Smith JA, Perusinghe N, Monoghan P (1986) Cell proliferation in the human mammary epithelium. Differential contribution by epithelial and myoepithelial cells. Am J Pathol 124(2):199–206

Jung F, Palmer LA, Zhou N, Johns RA (2000) Hypoxic regulation of inducible nitric oxide synthase via hypoxia inducible factor-1 in cardiac myocytes. Circ Res 86(3):319–325

Lakhani SR, O'Hare MJ (2001) The mammary myoepithelial cell–Cinderella or ugly sister? Breast Cancer Res 3(1):1–4

Lala PK, Orucevic A (1998) Role of nitric oxide in tumor progression: lessons from experimental tumors. Cancer Metastasis Rev 17(1):91–106

Le QT, Denko NC, Giaccia AJ (2004) Hypoxic gene expression and metastasis. Cancer Metastasis Rev 23(3–4):293–310

Liao D, Corle C, Seagroves TN, Johnson RS (2007) Hypoxia-inducible factor-1alpha is a key regulator of metastasis in a transgenic model of cancer initiation and progression. Cancer Res 67(2):563–572

Liu QY, Niranjan B, Gomes P, Gomm JJ, Davies D, Coombes RC, Buluwela L (1996) Inhibitory effects of activin on the growth and morphogenesis of primary and transformed mammary epithelial cells. Cancer Res 56(5):1155–1163

Liu L, Sun L, Zhao P, Yao L, Jin H, Liang S, Wang Y, Zhang D, Pang Y, Shi Y, Chai N, Zhang H, Zhang H (2010) Hypoxia promotes metastasis in human gastric cancer by up-regulating the 67-kDa laminin receptor. Cancer Sci 101(7):1653–1660

Loibl S, Buck A, Strank C, von Minckwitz G, Roller M, Sinn HP, Schini-Kerth V, Solbach C, Strebhardt K, Kaufmann M (2005) The role of early expression of inducible nitric oxide synthase in human breast cancer. Eur J Cancer 41(2):265–271

Margheri F, Luciani C, Taddei ML, Giannoni E, Laurenzana A, Biagioni A, Chilla A, Chiarugi P, Fibbi G, Del Rosso M (2014) The receptor for urokinase-plasminogen activator (uPAR) controls plasticity of cancer cell movement in mesenchymal and amoeboid migration style. Oncotarget 5(6):1538–1553

Montrucchio G, Lupia E, de Martino A, Battaglia E, Arese M, Tizzani A, Bussolino F, Camussi G (1997) Nitric oxide mediates angiogenesis induced in vivo by platelet-activating factor and tumor necrosis factor-alpha. Am J Pathol 151(2):557–563

Nagle RB, Bocker W, Davis JR, Heid HW, Kaufmann M, Lucas DO, Jarasch ED (1986) Characterization of breast carcinomas by two monoclonal antibodies distinguishing myoepithelial from luminal epithelial cells. J Histochem Cytochem 34(7):869–881

Nguyen M, Lee MC, Wang JL, Tomlinson JS, Shao ZM, Alpaugh ML, Barsky SH (2000) The human myoepithelial cell displays a multifaceted anti-angiogenic phenotype. Oncogene 19(31):3449–3459

Perou CM, Jeffrey SS, van de Rijn M, Rees CA, Eisen MB, Ross DT, Pergamenschikov A, Williams CF, Zhu SX, Lee JC, Lashkari D, Shalon D, Brown PO, Botstein D (1999) Distinctive gene expression patterns in human mammary epithelial cells and breast cancers. Proc Natl Acad Sci USA 96(16):9212–9217

Perou CM, Sorlie T, Eisen MB, van de Rijn M, Jeffrey SS, Rees CA, Pollack JR, Ross DT, Johnsen H, Akslen LA, Fluge O, Pergamenschikov A, Williams C, Zhu SX, Lonning PE, Borresen-Dale AL, Brown PO, Botstein D (2000) Molecular portraits of human breast tumours. Nature 406(6797):747–752

Radisavljevic Z (2004) Inactivated tumor suppressor Rb by nitric oxide promotes mitosis in human breast cancer cells. J Cell Biochem 92(1):1–5

Rehm S (1990) Chemically induced mammary gland adenomyoepitheliomas and myoepithelial carcinomas of mice. Immunohistochemical and ultrastructural features. Am J Pathol 136(3):575–584

Reveneau S, Arnould L, Jolimoy G, Hilpert S, Lejeune P, Saint-Giorgio V, Belichard C, Jeannin JF (1999) Nitric oxide synthase in human breast cancer is associated with tumor grade, proliferation

rate, and expression of progesterone receptors. Lab Invest 79(10):1215–1225

Ridnour LA, Thomas DD, Switzer C, Flores-Santana W, Isenberg JS, Ambs S, Roberts DD and Wink DA (2008) Molecular mechanisms for discrete nitric oxide levels in cancer. Nitric Oxide 19(2):73–76. doi:10.1016/j.niox.2008.04.006

Rudland PS, Fernig DG, Smith JA (1995) Growth factors and their receptors in neoplastic mammary glands. Biomed Pharmacother 49(9):389–399

Santosh R, Padu K, Singh ThB, Sharma MB, Singh TS (2013) Myoepithelial carcinoma of the breast. J Clin Diagn Res 7(6):1191–1193

Solinas G, Germano G, Mantovani A, Allavena P (2009) Tumor-associated macrophages (TAM) as major players of the cancer-related inflammation. J Leukoc Biol 86(5):1065–1073

Sollid J, Rissanen E, Tranberg HK, Thorstensen T, Vuori KA, Nikinmaa M, Nilsson GE (2006) HIF-1alpha and iNOS levels in crucian carp gills during hypoxia-induced transformation. J Comp Physiol B 176(4):359–369

Sternlicht MD, Kedeshian P, Shao ZM, Safarians S, Barsky SH (1997) The human myoepithelial cell is a natural tumor suppressor. Clin Cancer Res 3(11):1949–1958

Thomas DD, Ridnour LA, Isenberg JS, Flores-Santana W, Switzer CH, Donzelli S, Hussain P, Vecoli C, Paolocci N, Ambs S, Colton CA, Harris CC, Roberts DD, Wink DA (2008) The chemical biology of nitric oxide: implications in cellular signaling. Free Radic Biol Med 45(1):18–31

Thomsen LL, Miles DW (1998) Role of nitric oxide in tumour progression: lessons from human tumours. Cancer Metastasis Rev 17(1):107–118

Urtreger AJ, Aguirre Ghiso JA, Werbajh SE, Puricelli LI, Muro AF, de Kier Bal, Joff E (1999) Involvement of fibronectin in the regulation of urokinase production and binding in murine mammary tumor cells. Int J Cancer 82(5):748–753

Wang GL, Semenza GL (1993) Desferrioxamine induces erythropoietin gene expression and hypoxia-inducible factor 1 DNA-binding activity: implications for models of hypoxia signal transduction. Blood 82(12):3610–3615

Wang GL, Jiang BH, Rue EA, Semenza GL (1995) Hypoxia-inducible factor 1 is a basic-helix-loop-helix-PAS heterodimer regulated by cellular O2 tension. Proc Natl Acad Sci USA 92(12):5510–5514

Williams-Fritze MJ, Carlson Scholz JA, Bossuyt V, Booth CJ (2011) Use of p63, a myoepithelial cell marker, in determining the invasiveness of spontaneous mammary neoplasia in a rhesus macaque (*Macaca mulatta*). J Am Assoc Lab Anim Sci 50(2):252–257

Xiao G, Liu YE, Gentz R, Sang QA, Ni J, Goldberg ID, Shi YE (1999) Suppression of breast cancer growth and metastasis by a serpin myoepithelium-derived serine proteinase inhibitor expressed in the mammary myoepithelial cells. Proc Natl Acad Sci USA 96(7):3700–3705

Xu J, Xu X, Verstraete W (2000) Adaptation of *E. coli* cell method for micro-scale nitrate measurement with the Griess reaction in culture media. J Microbiol Methods 41(1):23–33